Journal of the Korean Institute of Electrical and Electronic Material Engineers, Vol. 15, No. 10, p. 914, October 2002.

논 문 15-10-14

Fabrication of Dual-mode Ultrasonic Transducer using PZT

Yeon-Bo Kim* and Yong-Rae Rho**

Abstract

This study investigates the mechanism of a dual mode probe that generates both of the longitudinal and shear waves simultaneously with a single PZT element. Most of conventional ultrasonic probes are constructed to generate either longitudinal or shear waves. After poling, PZT has the hexagonal 6mm crystal symmetry. All possible crystal cuts are checked to determine appropriate Euler transformation angles for efficient excitation of dual modes. For the selected cut, performance of the dual mode element is analyzed through numerical simulation and experiments. Results of the analysis determine the optimal crystal cut for simultaneous generation of P and S waves of equal strength.

Key Words: Dual mode ultrasonic probes, PZT, Impedance analysis, Pulse-echo simulation

1. INTRODUCTION

Ultrasonic probes are normally used to generate either longitudinal or shear waves in a medium. However, ultrasonic material characterization often requires the measurement of both longitudinal and shear wave properties. In such cases, ultrasonic probes that can generate both of above mentioned waves would be of great use. As one of the case, in nondestructive evaluation of metal welding, ultrasonic waves reflected from inherent cracks go through many mode conversions causing complex waves motions. The reliability of intergranular stress corrosion crack detection and the accuracy of discontinuity sizing are limited by the scattering and skewing of ultrasonic waves near the dissimilar metal interfaces at the welded zone. This limitation exists especially for pipes with or without corrosion resistant cladding on the inside surface or weld overlay on the outside surface[1]. Single mode ultrasonic probes producing either shear or longitudinal waves do not use all the information available to detect, confirm the size tight and branched intergranular stress corrosion cracks. These facts motivate the study in this paper.

This study is aimed at developing dual mode probes that can generate both of P/S (longitudinal and shear) waves efficiently. Several works have been done on the development of the P/S mode probes and the simultaneous excitation phenomenon has been confirmed both theoretically and experimentally. [2,3] By rotating the crystal axes, they could obtain the dual mode. However, most of the work have focused on just proof of the feasibility. The efficiency of the probe has not been fully explored. Transduction efficiency of the crystal is a function of the amount of crystal axis rotation because piezoelectric materials are inherently anisotropic. The purpose of the dual-mode probe is to generate or receive

* : School of Computer and Communiaction, Daegu University
(15, Naeriri, Jinryang, Kyungsan, Kyungpook, Fax: 053-850-6619
E-mail: ybkim@daegu.ac.kr)
** : Dept. of Mechanical Engineering, Kyungpook National University
Received April, 18, 2002. Accepted July, 12, 2002

both of waves equally well. In other words, the dual mode probe should allocate equal amount of input electrical energy to each type of the wave and vice versa. For that purpose, the angle of crystal axis rotation should be carefully determined because transduction efficiency ratio for each of waves is heavily dependent on the angle. If the angle is selected arbitrarily, generated waves will be either more longitudinal or more shear, and will not meet the requirement of dual mode of equi-strength. In this paper, we investigated the performance of a PZT element as a function of the rotation angle so that its efficiency was optimized to excite two waves equally strongly. Validity of the results is verified through analysis of impedance and performance variation of the probe both theoretically and experimentally. Finite element method is employed for theoretical analysis of the impedance variation.

2. THEORY

Piezoceramic PZT has the 6mm crystal symmetry, and has 10 independent material constants (5 stiffness constants, 3 piezoelectric constants, and 2 dielectric constants). For typical PZT disk elements, poling direction is normal to the disk surface, that is, crystal Z axis is normal to the surface. Depending on the desired type wave, orientation of the crystal axis must be carefully selected. It is known that, along each such orientation, one longitudinal (pure or quasi) and two shear (pure or quasi) modes may be excited. Our purpose is to check the effect of the orientation on the efficiency of simultaneous excitation of all waves. Hence, the crystal axes X, Y and Z are transformed with respect to the geometrical coordinate axis x, y and z with arbitrary Euler angles. Transformation is carried out by the well-known orthogonal coordinate rotation law[4]. According to Ref. 2, the simultaneous generation of P/S modes is possible only when the crystal Z axis is rotated with respect to crystal X or Y axis. The crystal plane normal to the poling direction is isotropic. Rotation with respect to either X axis or Y axis does not make any difference. When the crystal Z axis is rotated with respect to the crystal X axis, Fig. 1, the matrices of material constants take the following form.

$$[c^E] = \begin{bmatrix} c_{11}^E & c_{12}^E & c_{13}^E & c_{14}^E & 0 & 0 \\ c_{12}^E & c_{22}^E & c_{23}^E & c_{24}^E & 0 & 0 \\ c_{13}^E & c_{23}^E & c_{33}^E & c_{34}^E & 0 & 0 \\ c_{14}^E & c_{24}^E & c_{34}^E & c_{44}^E & 0 & 0 \\ 0 & 0 & 0 & 0 & c_{55}^E & c_{56}^E \\ 0 & 0 & 0 & 0 & c_{56}^E & c_{66}^E \end{bmatrix}$$

$$[e] = \begin{bmatrix} 0 & 0 & 0 & 0 & e_{15} & e_{16} \\ e_{21} & e_{22} & e_{23} & e_{24} & 0 & 0 \\ e_{31} & e_{31} & e_{33} & e_{34} & 0 & 0 \end{bmatrix} \qquad (1)$$

$$[\varepsilon^S] = \begin{bmatrix} \varepsilon_{11}^S & 0 & 0 \\ 0 & \varepsilon_{22}^S & \varepsilon_{23}^S \\ 0 & \varepsilon_{23}^S & \varepsilon_{33}^S \end{bmatrix}$$

, where $[C^E]$ is the stiffness matrix measured at constant electric field, $[e]$ is the piezoelectric matrix, and $[\varepsilon^S]$ is the dielectric matrix measured at constant strain. When an ultrasonic wave propagates into a piezoelectric material, it should satisfy the well-known Christoffel tensor equation[5].

$$\left[C_{ijkl}^E n_k n_j + \frac{(e_{ijk} n_k n_j)(e_{ikl} n_k n_i)}{\varepsilon_{ik}^S n_i n_j} \right] U_l = \rho v^2 U_i \qquad (2)$$

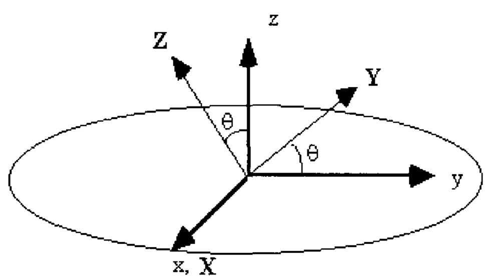

Fig. 1. Rotation of crystal Y and Z axes with respect to crystal X axis. x, y and z are geometrical axes.

where ρ is the density of the crystal, v is the wave velocity, U_i is the displacement, and n_i is the unit vector. When these material constants in Eq. (1) are put into the Christoffel equation in a matrix form, we can get wave velocities as Eq. (3), (4) and (5) after some algebra.

$$\rho v^2 U_x = c_{55}^E U_x \tag{3}$$

$$\rho v^2 U_y = \frac{1}{2}\left[\left(c_{44}^E + c_{33}^E + \frac{e_{34}^2}{\varepsilon_{33}^S} + \frac{e_{33}^2}{\varepsilon_{33}^S} \right) - \sqrt{ \left(c_{44}^E - c_{33}^E + \frac{e_{34}^2}{\varepsilon_{33}^S} + \frac{e_{33}^2}{\varepsilon_{33}^S} \right)^2 + 4\left(c_{43}^E + \frac{e_{34} e_{33}}{\varepsilon_{33}^S} \right)^2 } \right] U_y \tag{4}$$

$$\rho v^2 U_z = \frac{1}{2}\left[\left(c_{44}^E + c_{33}^E + \frac{e_{34}^2}{\varepsilon_{33}^S} + \frac{e_{33}^2}{\varepsilon_{33}^S} \right) + \sqrt{ \left(c_{44}^E - c_{33}^E + \frac{e_{34}^2}{\varepsilon_{33}^S} + \frac{e_{33}^2}{\varepsilon_{33}^S} \right)^2 + 4\left(c_{43}^E + \frac{e_{34} e_{33}}{\varepsilon_{33}^S} \right)^2 } \right] U_z \tag{5}$$

In these equations, values of all material constants except density are functions of the crystal axis rotation angle, θ in Fig. 1. Of these three waves, Eq. (3) is a pure shear wave that can not be excited by an external electric signal, hence of no value for transduction purposes. Eq. (4) is the quasi-shear wave and Eq. (5) is the quasi-longitudinal wave in that normal and transverse material constants are coupled with each other. These equations confirm the fact that we can generate both the longitudinal and the shear wave with a single element of PZT, once it is rotated appropriately. Velocities from Eqs. (4) and (5) can be written in terms of electromechanical coupling factors for each case as follows,

$$\begin{aligned} v_{ps}^2 &= v_{pu}^2 (1 + k_p^2) \\ v_{ss}^2 &= v_{su}^2 (1 + k_s^2) \end{aligned} \tag{6}$$

, where v_{ps}, v_{pu} and k_p^2 are stiffened, unstiffened velocities of the quasi-longitudinal wave, and the corresponding coupling factor, while v_{ss}, v_{su} and k_s^2 are stiffened, unstiffened velocities of the quasi-shear wave and the corresponding coupling factor. The unstiffened velocity is calculated from Eqs. (4) and (5) by setting all piezoelectric constants to zero. Our purpose is to check the effect of the amount of rotation on the excitation efficiency. The excitation efficiency is by definition proportional to the coupling factor denoted in Eq. (7) derived from the Eq. (6).

$$\begin{aligned} k_p^2 &= \frac{v_{ps}^2}{v_{pu}^2} - 1 \\ k_s^2 &= \frac{v_{ss}^2}{v_{su}^2} - 1 \end{aligned} \tag{7}$$

We employ PZT-5H as the piezoelectric material, because it is widely used for ultrasonic probes, and is easily available. With substitution of properties of the PZT-5H in Table 1 into the Eq. (7), we get the variation of the coupling factors k_p^2 and k_s^2 with the counter-clockwise rotation angle θ as in Fig. 2.

The material constant of PZT-5H in the Table 1 is for the case when crystal Z axis (poling direction) is parallel to the coordinate z axis (normal of the PZT disk). According to

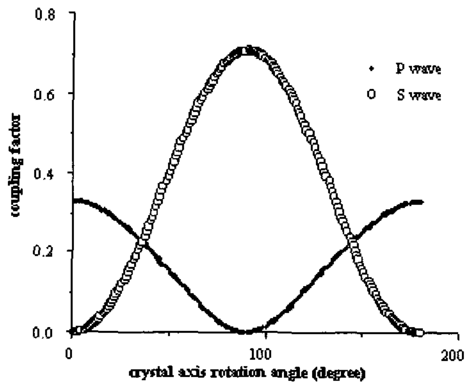

Fig. 2. Variation of the coupling factor k^2 with crystal Z axis rotation.

the figure, when the Z axis is coincident with the coordinate z axis ($\theta=0°$, the element generates longitudinal waves only, while when it is coincident with coordinate y axis ($\theta=90°$, the element generates shear waves only. On the other hand, $30°$ rotated PZT element gives both of the P/S waves while putting more emphasis on the longitudinal wave, and $45°$ rotated element generates stronger shear waves with relatively weaker longitudinal waves. The figure shows that when the crystal Z axis is rotated $35.7°$, the PZT element takes equal efficiency in exciting each of the longitudinal and shear waves. Hence the rotation angle of $35.7°$ is the optimum crystal axis direction at which the P and S waves have equal strength. In practice, even though the PZT element generates P and S waves of equi-strength, there is no guarantee that still equally strong P and S waves propagate through an acoustic radiation medium. The impedance mismatch, if any, between the PZT element and radiation medium can cause

Table 1. Properties of the material in the simulation of a dual mode ultrasonic transducer.

PZT	C_{11}^E	126 Gpa
	C_{12}^E	79.5 Gpa
	C_{13}^E	84.1 Gpa
	C_{33}^E	117 Gpa
	C_{44}^E	23.0 Gpa
	e_{15}	17.03 C/m^2
	e_{31}	-6.53 C/m^2
	e_{33}	23.3 C/m^2
	$\varepsilon_{11}^S/\varepsilon_o$	1,700
	$\varepsilon_{33}^S/\varepsilon_o$	1,400
	Density	7,500 kg/m^3
Steel	v_p	5,950 m/s
	v_s	3,210 m/s
	Density	57,830 kg/m^3
Epoxy resin	v_p	1,560 m/s
	v_s	720 m/s
	Density	2,500 kg/m^3

one type of these waves to suffer from more reflection than the other at the interface of two media. However, basically, the probe itself should be capable of exciting two type of waves with equal efficiency, and the impedance mismatch problem for each specific application can be solved by means of appropriate matching layers.

3. IMPEDANCE ANALYSIS

Validity of the above results is confirmed through experiment and finite element analysis (FEA) of the impedance variation of the PZT element with the rotation angle. The analysis is performed with a commercial package of FEA, ANSYS. The element type(SOLID 5) is selected to represent three-dimensional effects of the coupled fields (electrical and mechanical). Fig. 3 is a meshed model of the PZT square element for the FEA.

Thickness of the element is set arbitrarily to be 1 mm with lateral dimension of 10 mm, and material properties are those in Table 1. Fig. 4 is the impedance variation when the crystal normal is Z axis ($\theta=0°$) and Y axis ($\theta=90°$), respectively. They represent pure longitudinal and pure shear modes. The small ripples before the main resonance represent expanding modes and their harmonics (elongation and contraction modes in the length direction of the model).

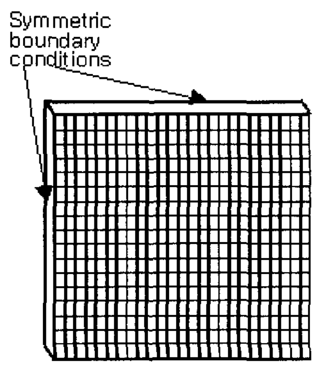

Fig. 3. Finite element mesh model of the PZT element.

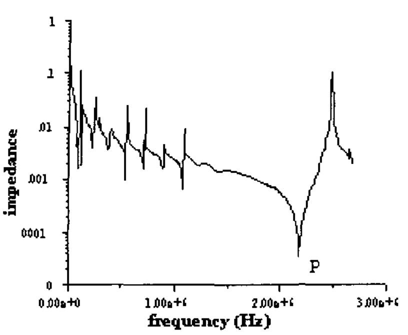

(a) pure longitudinal mode (Z axis normal)

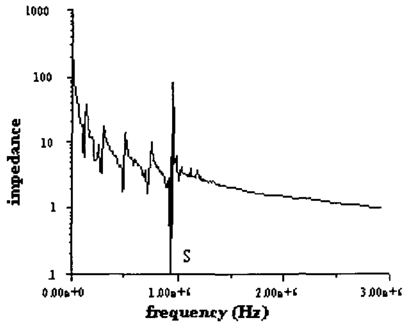

(b) pure shear mode (Y axis normal)

Fig. 4. Impedance variation of the PZT element with different crystal cut directions.

These two cases are the conventional use of PZT ceramics to fabricate either P mode or S mode probes. As observed in Sec. 2, when the normal of the crystal plane is placed in between these two, the element can excite both of P/S modes. Fig. 5 shows the impedance variation for the case of 30°, 35.7° and 45° counter-clockwise rotation. We can see that the resonance of the shear mode gets more and more prominent as the rotation angle increases. For now, it is not clear to see that 35.7° is the optimum rotation angle for the P/S waves of equi-strength. Confirmation of the optimality can be checked through pulse-echo tests that are to be done in the consecutive section. The results of Fig. 5 are checked experimentally. The rotation of 35.7°, Fig. 5(b), is not easy to achieve in practice. For this feasibility study, only the easier case, 30° and 45°, are worked out. Samples are PZT-5H from Murata, Japan. Measurement results are shown in Fig. 6. They

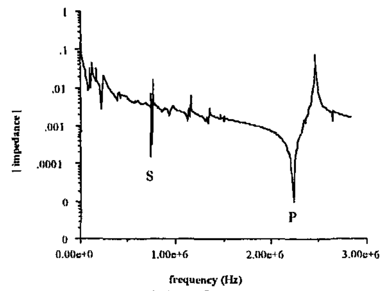

(a) 30° rotation.

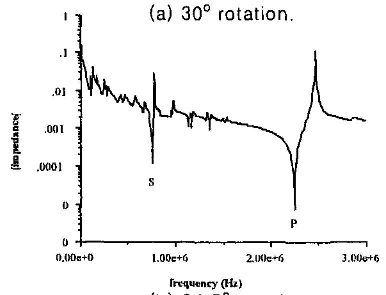

(b) 35.7° rotation.

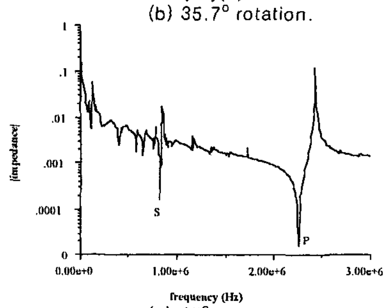

(c) 45° rotation.

Fig. 5. Variation of impedance analyzed with finite element method.

confirm the theoretic prediction. Resonant peaks show different forms from each other, which proves the dependency of the efficiency on the rotation angle. As expected, the result of 45° rotation shows a more pronounced resonance of the shear mode. Discrepancy in values of the resonance frequencies from those of the theoretical simulation is due to the difference of sample thickness between the FEA (1[mm]) and experiments (0.9[mm]).

4. PULSE-ECHO SIMULATION

Optimality of the dual mode generation is checked through theoretical pulse-echo modeling that simulates delay line measurement with the probe. The simulation employs the algorithm in Ref. [6]. Fig. 7 describes the schematic diagram of delay line measurement for the simulation. The delay line material is set to be steel because the probe under study is for use in nondestructive testing where most of target samples are metallic material. The backing material at the backside of the PZT is epoxy resin that absorbs backward waves to prevent spurious signals. Table 1 shows material properties used in the simulation.

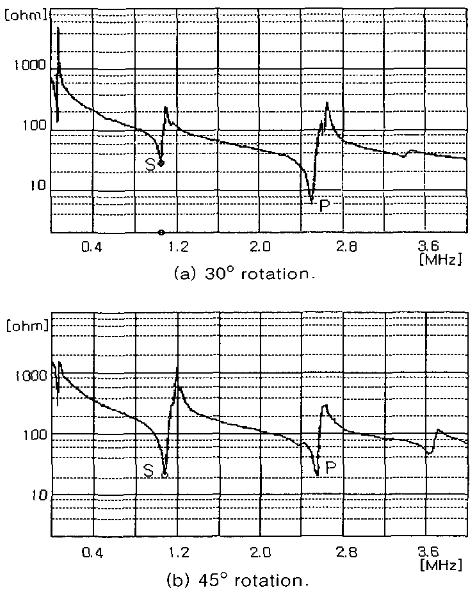

Fig. 6. Variation of impedance analyzed through experiments.

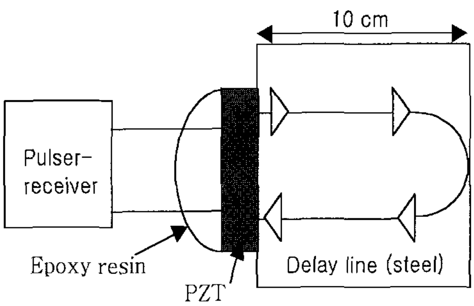

Fig. 7. Schematic diagram of the delay line measurement for the numerical simulation.

Fig. 8 is the simulation results. As expected, for all cases, both P and S waves are generated, and, due to the velocity difference, the P wave precedes the S wave. As the inclination angle of the crystal cut increases, the amplitude of the P wave decreases while that of the S wave increases. At the rotation angle of 30°, the amplitude of the P wave is larger than that of the S wave, while at the angle of 45°, the amplitude of the S wave is much larger than that of the P wave. On the other hand, at 35.7°, amplitudes of both P and S waves are quite similar, though the P wave amplitude is still a little bit larger than the S wave. This result in general confirms the expectation of

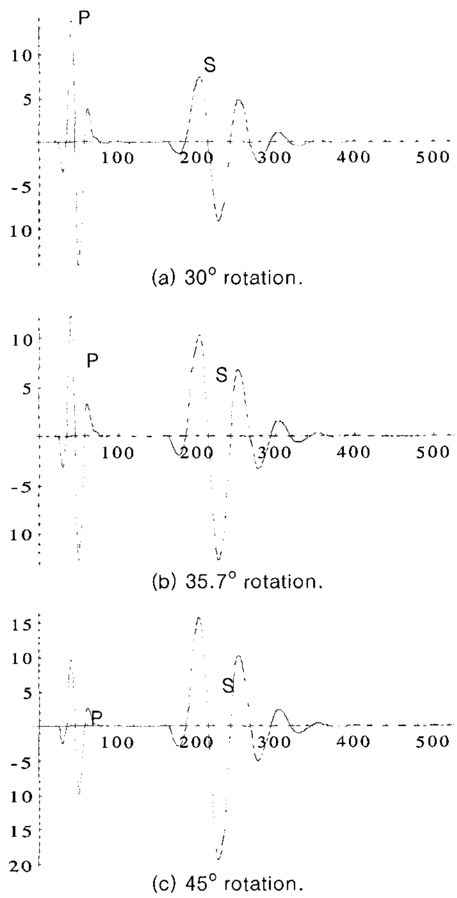

Fig. 8. Pulse-echoed waves for each rotation angle.

previous sections. However, the amplitudes at the optimum angle are not identical. That is considered due to the difference of acoustic impedance between the PZT and steel.

At the $35.7°$ rotation, the ratio of acoustic longitudinal impedance of the steel and the PZT is 0.73, and is larger than that of acoustic shear impedance (0.53). That means that the reflection coefficient of the S wave at the interface of the delay line and the PZT is larger than that of the P wave. Even though the amplitude of the P and S waves generated by the PZT is identical, the pulse-echoed S wave suffers from more reflection, i.e. energy loss, than the P wave, and resultant amplitudes show the difference. If the delay line is made of other material, for example of longitudinally harder material, the S wave may show larger amplitude. We are developing a general purpose transducer, not for a specific application. Therefore, considering that the target can be made of various materials in practice, the design scheme in this paper is still valid and more general. For a specific application, we can attach appropriate matching layers in front of the PZT element and relieve the impedance mismatch phenomenon. Therefore, the above pulse-echo simulation results can be said to confirm the fact that at the rotation angle of $35.7°$, both of the P and S waves are excited equally strongly.

5. CONCLUSION

We have investigated the mechanism of a dual mode probe that can generate both of longitudinal and shear waves simultaneously with a single PZT element. The efficiency of the dual mode excitation is dependent on the orientation of crystal axes. For PZT disk samples, as the crystal Z axis is rotated counter-clockwise from the normal to the disk surface, it gets more efficient in exciting shear waves. The results have been confirmed through impedance analysis and pulse-echo simulation. The rotation angle of $35.7°$ has been found to provide equal efficiency in exciting two types of waves, and hence to be the optimal crystal axis direction for the dual mode probe. However, depending on specific applications, impedance mismatch between the PZT element and an acoustic radiation medium can cause discrepancy from the optimal condition, and that can be resolved by employing appropriate matching layers.

ACKNOWLEDGEMENT

This research was supported (in part) by the Daegu University Grant, 2001.

REFERENCES

[1] G. J. Gruber, G. J. Hendrix, and W. R. Schick, "Characterization of flaws in piping welds using satellite pulses", Materials EEvaluation, Vol. 42. p. 426, 1984.

[2] B. S. Kim, "A P/S mode transducer with a piezoelectric ceramic of PZT type: theory and fabrication", Materials Evaluation, Vol. 40, p. 186, 1982.

[3] J. Krautkramer and H. Krautkramer, "Ultrasonic Testing of Materials", Springer-Verlag, p. 117, 1990.

[4] J. F. Nye and F.R.S., "Physical Properties of Crystals", Oxford University Press, p. 9, 1985.

[5] B. A. Auld, "Acoustic Fields and Waves in Solids", John Wiley & Son(Vol. 1), p. 163, 1973.

[6] K. Yamaguchi, H. Yagami, and T. Fujii, "New method of time domain analysis of the performance of multilayered ultrasonic transducers", IEEE, Trans. on Ultrasonics, Ferroelectrics and Frequency Control, 33, p. 669, 1986.